Biomaterials Science

ROYAL SOCIETY OF CHEMISTRY

PAPER

View Article Online
View Journal | View Issue

Cite this: *Biomater. Sci.*, 2021, **9**, 3150

The role of lithium in the osteogenic bioactivity of clay nanoparticles†

Mohamed Mousa, [a] Juan Aviles Milan, [a] Oscar Kelly,[b] Jane Doyle,[b] Nicholas D. Evans, [a] Richard O. C. Oreffo [a] and Jonathan I. Dawson *[a]

Received 26th August 2020,
Accepted 5th March 2021

DOI: 10.1039/d0bm01444c

rsc.li/biomaterials-science

LAPONITE® clay nanoparticles are known to exert osteogenic effects on human bone marrow stromal cells (HBMSCs), most characteristically, an upregulation in alkaline phosphatase activity and increased calcium deposition. The specific properties of LAPONITE® that impart its bioactivity are not known. In this study the role of lithium, a LAPONITE® degradation product, was investigated through the use of lithium salts and lithium modified LAPONITE® formulations. In contrast to intact particles, lithium ions applied at concentrations equivalent to that present in LAPONITE®, failed to induce any significant increase in alkaline phosphatase (ALP) activity. Furthermore, no significant differences were observed in ALP activity with modified clay structures and the positive effect on osteogenic gene expression did not correlate with the lithium content of modified clays. These results suggest that other properties of LAPONITE® nanoparticles, and not their lithium content, are responsible for their bioactivity.

1. Introduction

A growing number of studies have reported the ability of clay nanoparticles to enhance osteogenic differentiation of skeletal stem and osteoprogenitor cell populations, even in the absence of traditional osteogenic supplements such as dexamethasone, ascorbate-2-phosphate and β-glycerophosphate. However, the mechanism(s) behind this osteogenic bioactivity remain poorly understood.[1] Relatively little attention has been given, for example, to the question of which specific properties of clay structure and composition play a role in imparting nanoclay bioactivity. Answering these questions is key for the successful control and manipulation of this exciting new class of biomaterial for therapeutic application.

Clay degradation products have been proposed as playing a role in clay osteogenic bioactivity.[2–8] For example, it has been suggested that following cellular uptake, clay nanoparticles may undergo degradation within the low pH endosomal or lysosomal intracellular compartments to release dissolution products known to influence osteogenic cell function.[2–8] In the case of LAPONITE®, these degradation products include orthosilicic acid $Si(OH)_4$, magnesium Mg^{2+}, and lithium Li^+ ions.[9,10] Orthosilicic acid $Si(OH)_4$ is known to promote collagen type 1 synthesis and osteoblast differentiation.[11] In studies of other magnesium containing biomaterials, released magnesium ions have been shown to activate osteogenesis-regulating pathways (HIF-1α and PGC-1α)[12,13] and are essential for integrin adhesion to biomaterial surfaces.[14] Perhaps most notable however is the potential influence of lithium on nanoclay bioactivity.

Lithium has garnered considerable attention for bone regenerative therapies due to its well-documented role in prompting osteogenesis and bone formation.[15,16] For example, a study conducted by Zamani *et al.*, reported that bone mineral density in several areas (the spine, the femoral neck and the trochanter) of 75 lithium-treated patients was significantly higher than that of normal participants,[17] and current use of lithium (in contrast to past use) was associated with a decreased risk of fracture.[18] Recently, Xu L *et al.*, reported the ability of lithium to enhance implant osseointegration, implant fixation, and bone formation in osteoporotic conditions,[19] suggesting lithium as a promising therapeutic agent for bone formation and preventing implant failure. *In vitro*, various studies have reported the ability of lithium to promote proliferation and osteogenic differentiation of bone marrow-derived stromal cells.[20–24]

These interesting osteogenic properties of lithium are mainly attributed to lithium's well-known pharmacological function as an agonist for the canonical Wnt signaling pathway[25] which plays a key role in modulating osteogenic gene expression. Lithium acts to inhibit glycogen synthase

[a]*Bone & Joint Research Group, Centre for Human Development, Stem Cells & Regeneration, Institute of Developmental Sciences, Faculty of Medicine, University of Southampton, Southampton, SO16 6YD, UK. E-mail: jid@soton.ac.uk*
[b]*BYK Additives Ltd., Moorfield Road, Widnes, Cheshire WA8 3AA, UK*

†Electronic supplementary information (ESI) available. See DOI: 10.1039/d0bm01444c

kinase 3 (GSK3β) from phosphorylating β-catenin, which subsequently escapes degradation and translocate to the nucleus to bind TCF/LEF transcription factor complex.[21,24–26] Aberrations or alterations in Wnt signaling pathway are known to lead to various osteogenic disorders in both animal and human models, which reflects not only its crucial role in normal bone physiology, but also the potential to modulate Wnt signalling as an attractive therapeutic target for bone regeneration.[26–29] For example, clinical trials using Wnt agonist drugs showed promising results augmenting bone formation and increasing bone mineral density[26,27] and incorporation of lithium ions in bioactive ceramics[23] and mesoporous bioglass[24] significantly enhanced proliferation and osteogenic differentiation of bone marrow stromal cells compared to lithium-free scaffolds.

In this study, we set out to test the hypothesis that lithium ions in LAPONITE® nanoclay are responsible for its bioactivity. After testing the direct influence of both lithium ions and LAPONITE® on luciferase activity of a Wnt reporter cell line, the osteogenic response of HBMSCs to lithium modified LAPONITE® analogues was explored by testing early and late markers of osteogenic differentiation. This investigation represents an opportunity not only to understand the role of lithium and Wnt signalling in LAPONITE® bioactivity, but may also lead to novel modified nanoclay structures able to tune specific cell responses for regeneration.

2. Results

2.1. LAPONITE® clay nanoparticles promote early osteogenic activity in human bone marrow stromal cells

Prior to examining the role of lithium modification in LAPONITE® bioactivity, the influence of standard LAPONITE® on viability and osteogenic differentiation of HBMSCs was investigated (Fig. 1). LAPONITE® exhibited no/negligible effects on the metabolic activity of HBMSCs over a range of cell seeding densities (1.5×10^3–12×10^3 cells per cm^2) up to a conc. of 100 μg mL^{-1} (Fig. 1A). However, higher clay doses, particularly at higher cell densities, led to a significant decrease in cell metabolic activity compared to control culture ($P = 0.0046$). Therefore, a working LAPONITE® conc. of 100 μg mL^{-1} was selected for subsequent experiments. F-Actin staining (FITC-phalloidin) confirmed normal cell spreading and morphology in the presence of Rhodamine B labelled LAPONITE® nanoparticles which appeared associated with the cells in monolayer cultures (Fig. 1B). Cells cultured with LAPONITE® (100 μg mL^{-1}) for 7 days prior to media change, showed a normal time-dependent increase in proliferation profile with no significant effect of LAPONITE® over the 14 day period (Fig. 1C).

The osteogenic bioactivity of LAPONITE® was evident by a time-dependent enhancement of alkaline phosphatase activity compared to the control (Fig. 1D). Alizarin red staining at day 14 (Fig. 1E) also revealed a strong enhancement in calcium deposition and the emergence of mineralised nodules with LAPONITE® addition (Fig. S1†) compared to the control which proved negative for calcium staining. Correspondingly, LAPONITE® addition significantly upregulated the expression of early osteogenic gene markers *ALPL* and *COL1A1* reaching around 15- and 3-fold increase, respectively, at day 3 (Fig. 1F). Interestingly, no significant increase in *RUNX2* mRNA levels was observed over the time frame tested and there was a significant reduction in the expression of Osterix (*SP7*; $P < 0.0001$). The late osteogenic markers osteopontin (*SPP1*) and osteocalcin (*BGLAP*) did not exhibit any significant response to LAPONITE® addition over the 7 day culture period.

2.2. LAPONITE® does not activate Wnt signalling and relevant concentrations of LAPONITE® degradation products do not promote osteogenic activity

LiCl addition caused a significant upregulation in TCF/LEF promoter activity in a Wnt luciferase reporter cell-line at ≥25 mM (Fig. 2A). In contrast, LAPONITE® addition at concentrations sufficient to enhance HBMSC ALP activity failed to induce any increase in luciferase reporter activity compared to the no-clay control (Fig. 2A and B). LiCl addition to HBMSCs at the concentrations required for promoter activity in the reporter cell line caused a dose-dependent down regulation of ALP activity over this range (Fig. 2C). Consistent with this and in contrast to *ALPL* gene expression, *AXIN2* expression was not upregulated in HBMSCs by LAPONITE® while being strongly upregulated by LiCl (Fig. 2D). Upregulation of *AXIN2* by LiCl was most marked after 24 hours, whereas *ALPL* and *COL1A1* upregulation by LAPONITE® increased over 48 hours. *RUNX2* expression was transiently downregulated at day 1 in response to both LAPONITE® and LiCl (Fig. S2†).

We also tested the effect on HBMSCs of lithium ions at the much lower 0.07–0.27 μg ml^{-1} (0.01–0.04 mM) concentration range that would be present following partial or complete degradation of LAPONITE® (25–100 μg ml^{-1}) in cell culture media. Silicon and magnesium ions were also tested at the relevant concentrations. In contrast to dispersed LAPONITE® nanoparticles, which caused a 20-fold increase in ALP activity ($P < 0.0001$) at the highest concentration, the three degradation products at their respective concentrations generated minimal effects on alkaline phosphatase activity. Only silicon caused a modest (1.3-fold) increase at the highest concentration tested, though, this effect was not apparent when normalised against the background of the relevant counter-ion (Fig. S3†). Lithium ions did not produce a significant change in HBMSC ALP activity over this range ($P = 0.0648$) (Fig. 2E).

2.3. Lithium-modification of LAPONITE® nanoparticles

The cellular uptake pathways and kinetics of ions are different when delivered in the form of nanoparticles.[30] Therefore, to further test the significance of lithium in LAPONITE® for osteogenesis, two structurally modified LAPONITE® analogues incorporating higher concentrations of lithium (HL) and null lithium (NL) were prepared. Additionally, to test the effect of adsorbed lithium on the bioactivity of LAPONITE®, a prepa-

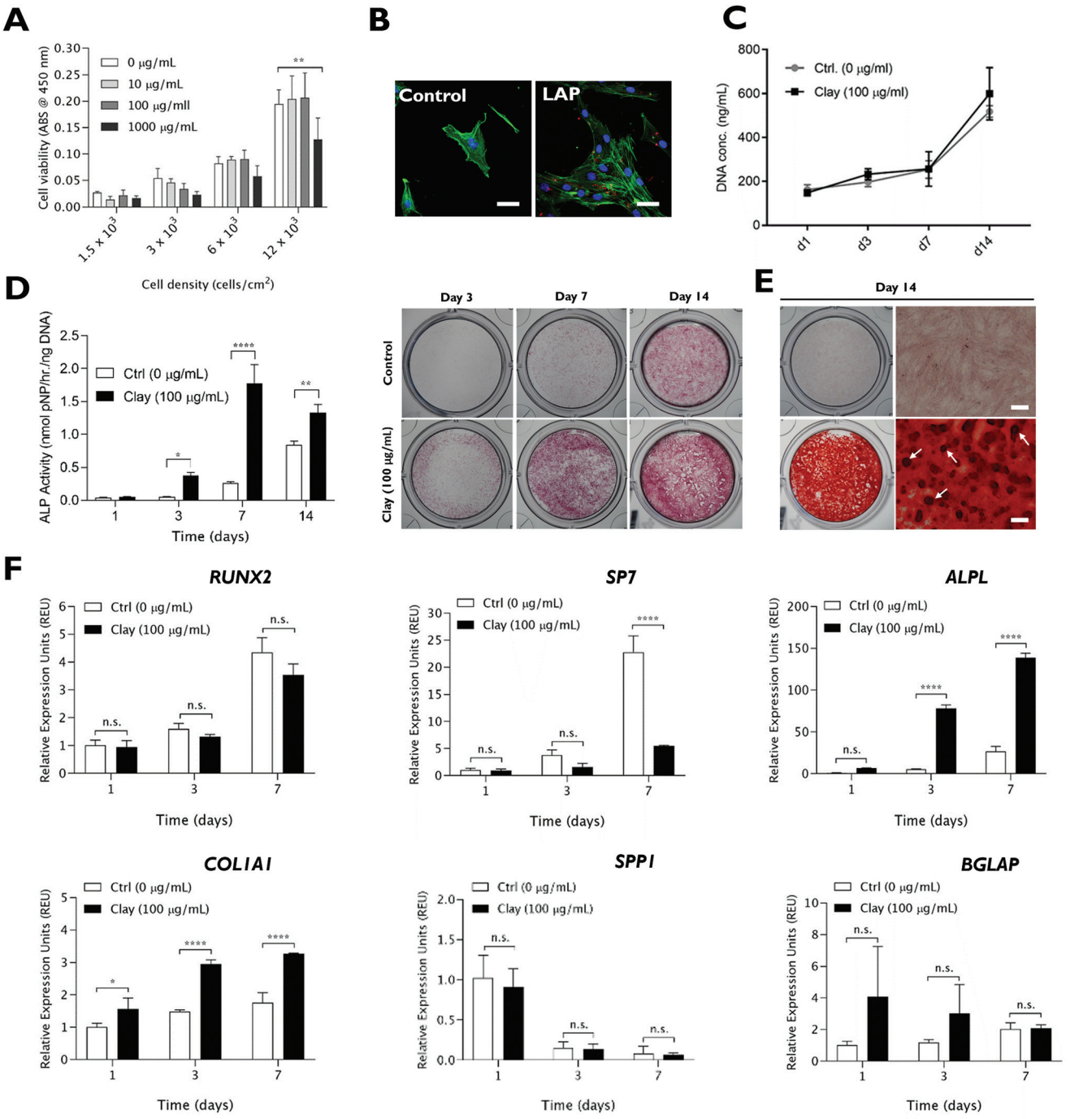

Fig. 1 Cytocompatibility and osteogenic bioactivity of LAPONITE® clay nanoparticles. (A) LAPONITE® clay nanoparticles, dispersed in cell culture media, are cytocompatible up to a concentration of 1 mg mL^{-1} as measured by WST1 assay at day 1 post-LAPONITE® addition. (B) Rhodamine B-labelled LAPONITE® NPs (100 µg mL^{-1}), added to HBMSCs for 24 hours, associate with cells in monolayer culture but do not interfere with cell adhesion and spreading as seen by staining of F-actin filaments (green). (C) Addition of LAPONITE® did not significantly alter the cell proliferation profile over 14 days. LAPONITE® nanoparticles (100 µg mL^{-1}) significantly enhanced ALP activity (D), calcified bone nodule formation (E) and upregulated expression of certain bone-related genes (F). Scale bar = 20 µm (B) and 400 µm (E). Statistical analysis was performed using two-way ANOVA followed by Tukey's multiple comparisons test. Data represent mean ± SD, $N = 3$ experimental replicates. *$P < 0.05$; $P < 0.01$; ****$P < 0.0001$; n.s. = non-significant.

ration of standard LAPONITE® with interlayer sodium ions exchanged for lithium (SL^{ex}) was also generated (Fig. 3A). XRD diffractograms confirmed that both standard and lithium modified clay minerals exhibited reflection peaks characteristic of pure LAPONITE® crystal without phase transformation or impurities (Fig. 3B).

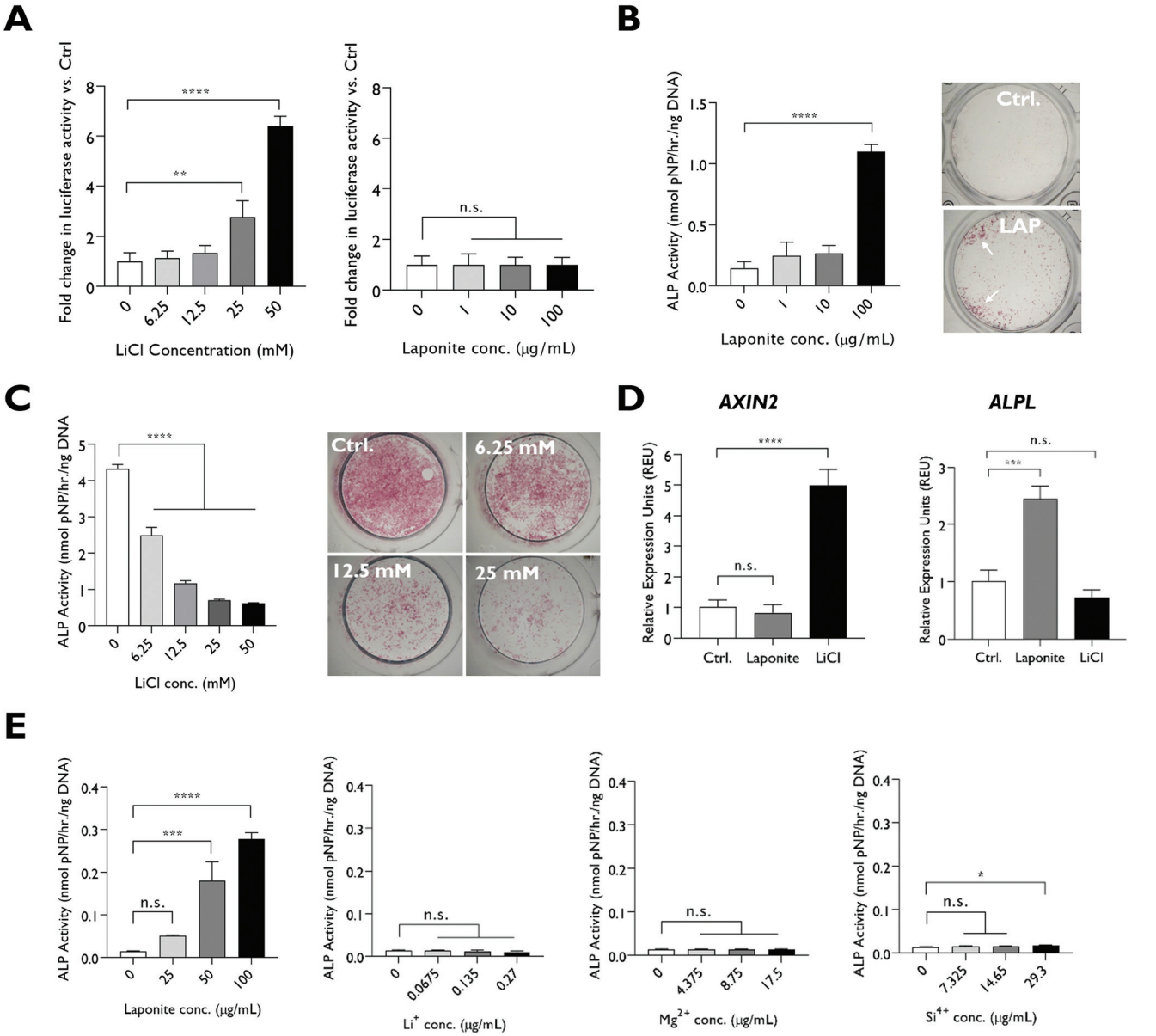

Fig. 2 Effect of lithium ions on osteogenic differentiation of HBMSCs through the canonical Wnt signaling pathway. (A) LiCl led to a significant dose-dependent increase in luciferase activity of a Wnt reporter cell line after 18 hours exposure while no significant effect on luciferase activity was observed with addition of LAPONITE®. (B) LAPONITE® significantly promoted ALP activity at 100 μg mL^{-1} as shown by ALP activity assay and ALP staining on day 3 whereas (C) LiCl addition to HBMSCs caused a dose-dependent decrease in ALP activity. (D) AXIN2 expression in HBMSCs was upregulated at day 2 by LiCl (50 mM) but not LAPONITE® (10 μg mL^{-1}), whereas ALPL gene expression was not upregulated by LiCl. In contrast to the strong dose dependent effects of dispersed LAPONITE® on ALP activity, LAPONITE® degradation products, including lithium, applied at concentrations equivalent to that present in LAPONITE® had minimal effects on alkaline phosphatase activity at day 3 with only silicon causing a slight increase at the highest concentration tested Statistical analysis was performed using one-way ANOVA followed by Tukey's multiple comparisons test. Data represent mean ± SD, $N = 3$ experimental replicates. $^{**}P < 0.01$; $^{***}P < 0.001$; $^{****}P < 0.0001$; n.s. = non-significant.

X-ray fluorescence (XRF), and atomic absorption spectroscopy (AAS) analysis (Fig. 3C) confirmed successful modification of lithium content in the octahedral sheets of HL and NL producing LAPONITE® analogues with structural lithium contents ranging from 0 to 5.5 mg g^{-1} in the order of HL > SL > NL. Efficient Na^+–Li^+ exchange reactions for the generation of $SL^{ex.}$ grade LAPONITE® were also confirmed by XRF and AAS which showed complete removal of Na^+ and a 2.6-fold increase in lithium concentration respectively.

2.4. Lithium content of LAPONITE® does not play a significant role in LAPONITE® osteogenic bioactivity

The effect of modifications in structural lithium on nanoclay osteogenic activity was investigated by incubating HBMSCs

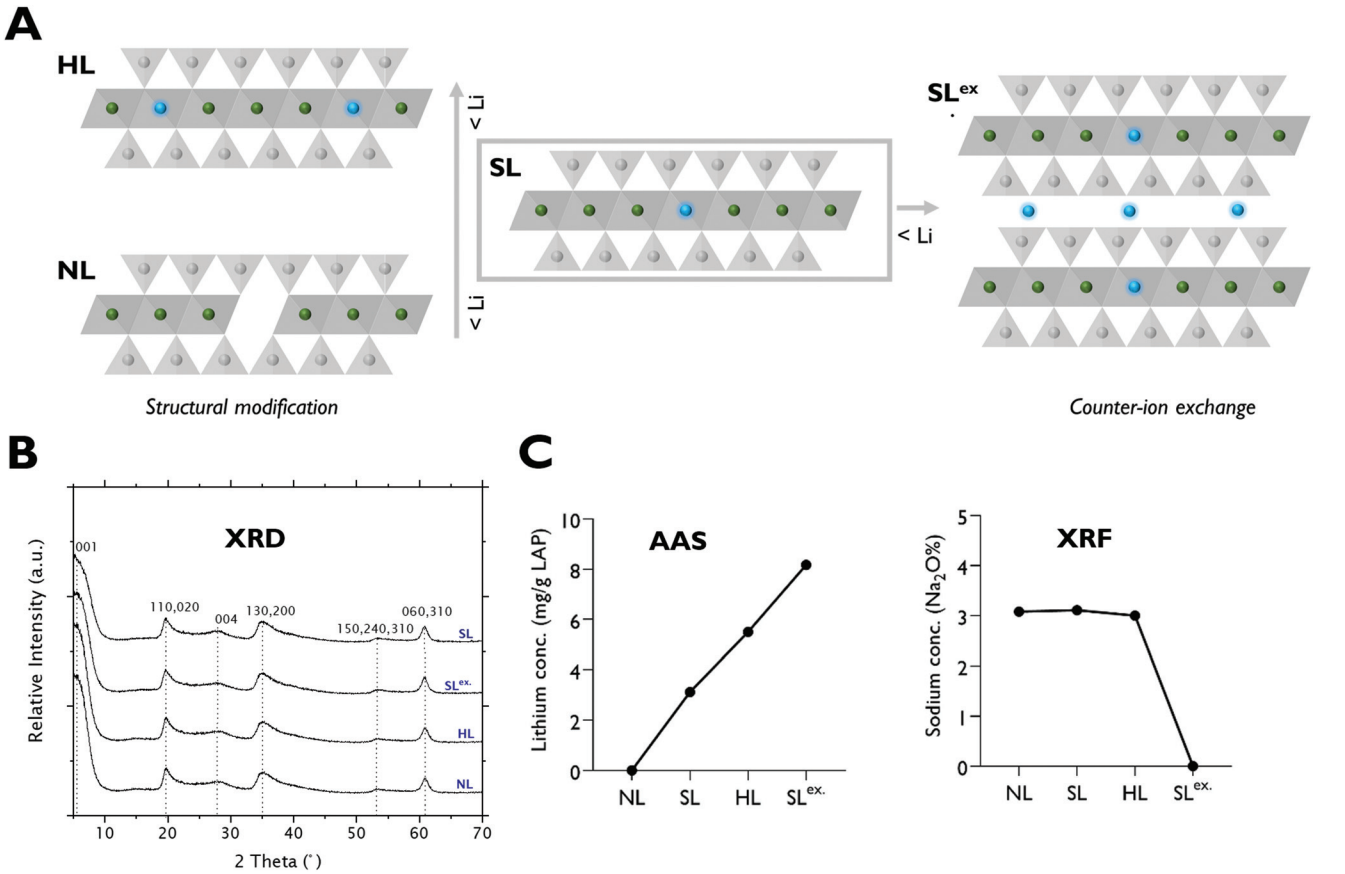

Fig. 3 Structural and compositional analysis of lithium modified clay nanoparticles. (A) Schematic of lithium modified LAPONITE® analogues (lithium ions represented in blue). (B) XRD diffractogram showing reflection peaks characteristic of pure Na-hectorite clay mineral without impurities or phase transformation compared to standard LAPONITE®. (B) Elemental analysis by XRF and AAS confirming successful modulation of clay lithium content.

with 100 μg ml^{-1} of each analogue for 7 days in basal media or media with standard osteogenic supplements (dexamethasone, ascrobate-2-phosphate and β-glycerophosphate). ALP activity was measured as an early osteogenic marker together with osteogenic gene expression (Fig. 4). Compared to the LAPONITE®-free control, all LAPONITE® analogues enhanced ALP activity of HBMSCs in osteogenic conditions ($P < 0.05$) but with no significant differences apparent between standard LAPONITE® and either of the modified clays (Fig. 4A). Overall, gene expression data did not provide clear evidence for a correlation between lithium content and LAPONITE® bioactivity. *ALPL* activity was significantly upregulated in basal conditions by HL ($P < 0.0001$) and SL ($P < 0.0001$) analogues, though interestingly not by NL ($P = 0.206$). However, this difference between clays was not apparent in osteogenic conditions where all analogues produced a significant and equivalent upregulation of *ALPL* ($P < 0.01$). Similarly, the significant increase in *COL1A1* expression across all clay analogues ($P < 0.01$) was slightly attenuated in the NL treatment ($P = 0.028$ compared with standard lithium) though again this difference was less apparent in osteogenic conditions ($P = 0.426$). None of the clay analogues caused an upregulation in *RUNX2* expression in either basal or osteogenic conditions. Finally, *SPP1*, while slightly increased by nanoclay addition in basal conditions (NL treatment, $P = 0.017$) was reduced compared to the control in osteogenic conditions (HL treatment, $P = 0.025$).

Exchange of the interlayer sodium for lithium did not significantly affect ALP activity (Fig. 5A) and, overall, the effect of SL^{ex} on osteogenic gene expression correlated closely with SL, the only exception being a slight but significant reduction in the strength of the upregulatory effect of LAPONITE® SL on *ALPL* in basal media (Fig. 5B). When fold change in gene expression was assessed against clay lithium content across all analogues (*cf.* Fig. 3C), no correlation was observed (Fig. 6).

3. Discussion and conclusion

Our goal in this study was to explore the role of lithium in the modulation of LAPONITE® nanoclay bioactivity. The bioactive

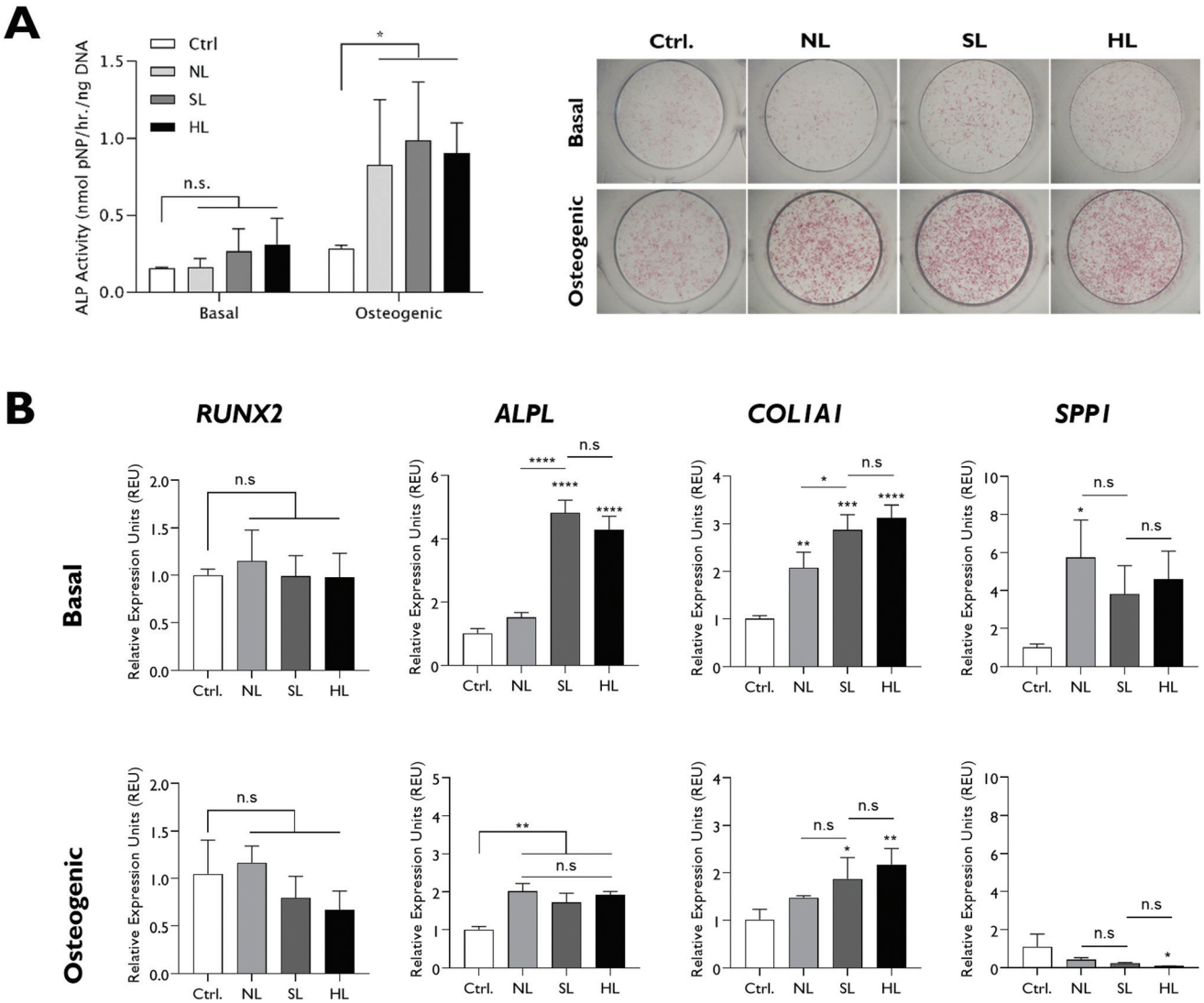

Fig. 4 Effect of structural lithium modifications on LAPONITE® osteogenic bioactivity assayed by ALP activity and osteogenic gene expression after 7 days (A) Both standard and modified structures promoted ALP activity of HBMSCs under osteogenic conditions compared to the no clay control but with no significant difference between the clay formulations. (B) All modified LAPONITE® analogues induced upregulation of *ALPL* and *COL1A1* gene expression compared to the no clay control in osteogenic conditions. In basal conditions this upregulation was reduced in the NL analogue. Statistical analysis was performed using one-way ANOVA followed by Tukey's multiple comparisons test. Data represent mean ± SD, $N = 3$. *$P < 0.05$; **$P < 0.01$; ***$P < 0.001$; ****$P < 0.0001$; n.s. = non-significant.

effect of LAPONITE® on osteogenic differentiation of skeletal populations has been widely reported[1–3,31–36] and observed both when applied as a dispersed additive to cell culture media[2,3,31,32] and as a composite in polymeric biomaterials.[5,33–36] In discussions of potential mechanisms in the literature it is frequently suggested that nanoclay bioactivity could be attributed to LAPONITE® degradation products.[2–8,31] Lithium is of particular interest in this context for its well-established pharmacological action as an agonist of the canonical Wnt pathway.

With the exception of day 14 assays for ALP activity and Alizarin red staining, all studies focused on the phenotypic effects that occurred over the first 7-days of exposure to LAPONITE® treatment prior to media change. This decision was based on two considerations: (1) the robust early upregulation of alkaline phosphatase in response to LAPONITE® is striking and warrants investigation into potential determinants upstream of this very early stage response. (2) The necessity for media change after seven days raises the question of whether or not to refresh the LAPONITE® or salts in the system. In either case, comparisons between the effects of nanoparticles, which may persist and/or accumulate, and salts which do not, become significantly more challenging after this time point.

The current studies confirmed that LAPONITE® clay nanoparticles, up to a concentration of 100 μg mL^{-1},

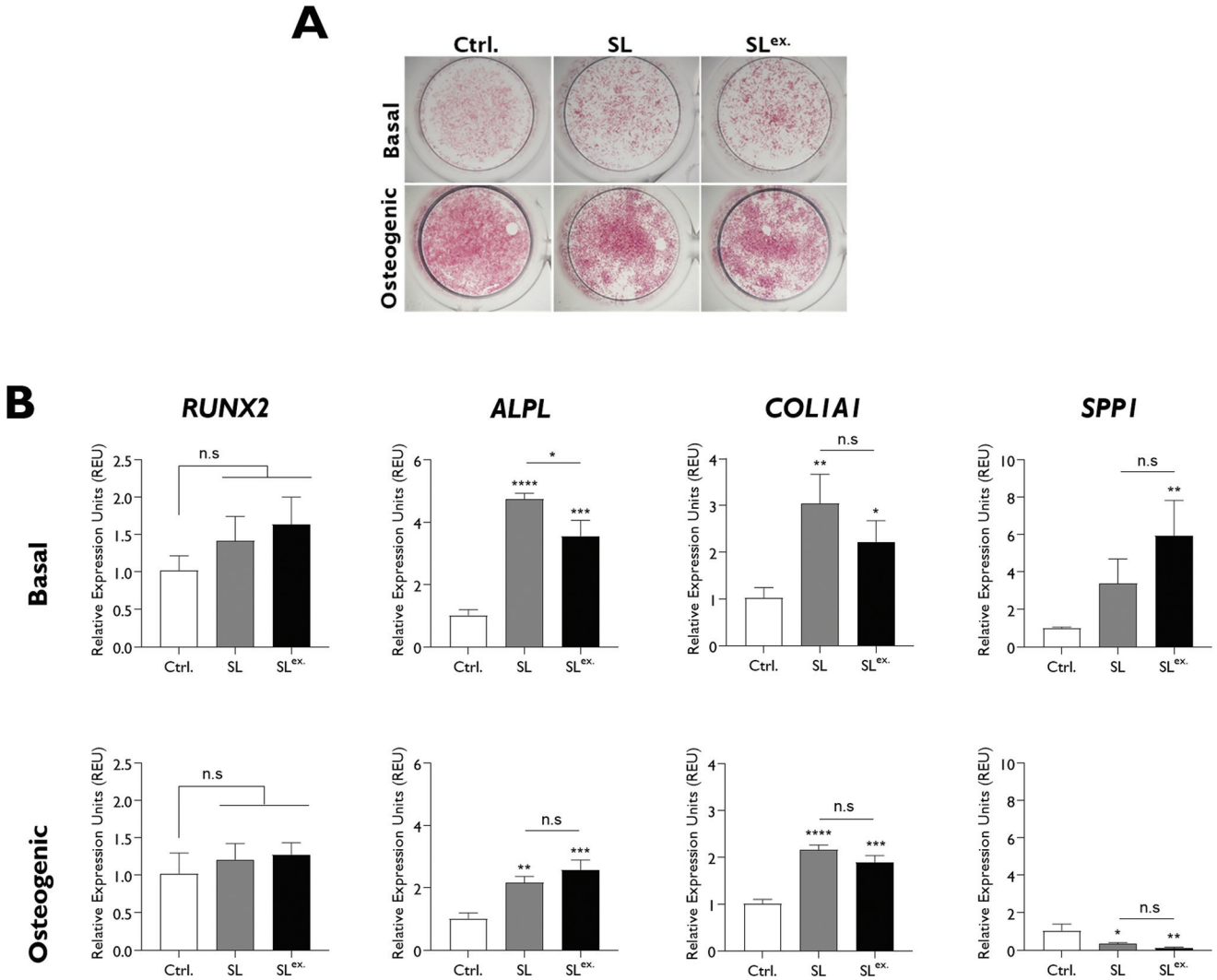

Fig. 5 Effect of exchanged lithium modification on LAPONITE® osteogenic bioactivity assayed by ALP activity and osteogenic gene expression after 7 days (A) No significant difference in ALP activity is apparent between standard and modified LAPONITE® structures in either basal or osteogenic cultures. (B) Both SL and SL^{ex} LAPONITE® analogues induced upregulation of *ALPL* and *COL1A1* gene expression compared to the no clay control in both basal and osteogenic conditions. In basal conditions this upregulation was reduced in the in the SL^{ex} treatment, though the SL^{ex} treatment produced a an enhanced significant effect on SPP1. Statistical analysis was performed using one-way ANOVA followed by Tukey's multiple comparisons test. Data represent mean ± SD, $N = 3$. *$P < 0.05$; **$P < 0.01$; ***$P < 0.001$; ****$P < 0.0001$; n.s. = non-significant.

robustly enhance certain bone-related phenotypic changes in HBMSCs without loss of viability. LAPONITE® nanoparticle addition caused a pronounced enhancement in ALP activity, calcium deposition and *ALPL* and *COL1A1* gene expression in agreement with previous studies.[1–3,5,31–36] Interestingly, genes for the principle osteogenic transcription factors, Runx2 and Osterix (*SP7*), were not upregulated in response to LAPONITE®, suggesting alternative signaling pathways lie behind the phenotypic changes observed. This observation is in contrast with some previous studies which describe upregulation of Runx2 with LAPONITE® addition,[2,3,32] although, notably, a whole transcriptome analysis of LAPONITE® effects on HBMSCs also recorded neither gene as being differentially expressed under similar conditions (*RUNX2*, false-discovery rate-adjusted $P = 0.519$ as calculated by authors from source dataset; *SP7*, undetermined).[31]

Regardless of the specificity of the response, the influence of LAPONITE® on the phenotype of HBMSCs does not appear to be mediated by the lithium content of LAPONITE® or involve the canonical Wnt pathway. Under equivalent conditions, LAPONITE® caused an upregulation of ALP activity but did not activate TCF/LEF, as demonstrated by both a Wnt reporter luciferase assay and Wnt-responsive gene expression, and whereas LiCl downregulated ALP at concentrations sufficient to activate TCF/LEF, it had no effect on ALP when added at the much lower concentrations present in LAPONITE®. While removal of structural lithium from

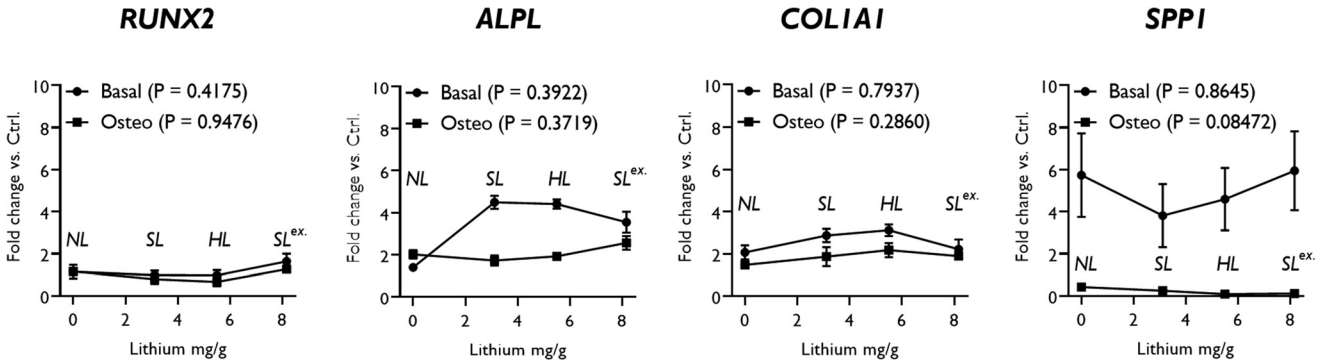

Fig. 6 LAPONITE® analogue effects on osteogenic gene expression by lithium content. Pearson's correlation coefficient analysis revealed no significant association between changes in osteogenic gene expression (fold change in expression over no clay control) and LAPONITE® lithium content in either osteogenic or basal conditions. *P* values for Pearson's analysis of each condition are presented in the legend. Annotations show which clay analogue each point along the *x*-axis represents.

LAPONITE® attenuated certain osteogenic effects, overall, lithium content of nanoclay analogues correlated poorly with expression of osteogenic markers.

LiCl caused a dose-dependent inhibition of ALP activity in HBMSCs at the concentrations sufficient for Wnt signaling activation. This reflects the complexity of the role of Wnt signaling in osteogenesis, which can promote or inhibit osteogenic differentiation depending on differentiation stage and co-factors present. For example studies by De Boer *et al.* and others[20,37] also report inhibitory effects under similar conditions. The amount of lithium present in LAPONITE® at the concentrations reported for its bioactivity (10–100 μg mL^{-1}) is much lower however and at these concentrations, as with each of the degradation products, failed to trigger a response in HBMSCs. Even assuming complete degradation – an unlikely scenario – lithium release from LAPONITE® would achieve a maximum concentration of 0.04 mM, which is 50× lower than the reported inhibition constant K_i of 2 mM for GSK3β enzyme activity[38,39] and 100× lower than the minimum reported osteogenic dose of lithium.[24] This fact alone suggests against a role for lithium in the osteogenic activity of LAPONITE®.

It is at least conceivable that the reported internalisation of LAPONITE®[31] and subsequent intra-cellular release of lithium upon degradation may elicit significantly different kinetics. To further explore the relationship between osteogenesis and LAPONITE® lithium therefore, LAPONITE® analogues modified for lithium content were generated and their effect on HBMSC osteogenic differentiation investigated. Overall, the results from these studies support the conclusion above that LAPONITE® osteogenic effects are not attributed to its lithium content. All LAPONITE® analogues tested, including null-lithium LAPONITE®, significantly enhanced ALP activity and *ALPL* and *COL1A1* gene expression in osteogenic conditions relative to the clay-free control. Overall, fold-changes in all genes correlated poorly with nanoclay lithium content. These findings are consistent with a growing body of literature that indicate such osteogenic effects *in vitro* to be a more generalised feature of clays – many of which do not contain lithium. For example, Kim *et al.* showed that dispersion of MMT ($Na_m(Al_{2-m}Mg_m)Si_4O_{10}(OH)_2{\cdot}nH_2O$) nanoparticles in cell culture media enhanced ALP activity, mineralization and expression of osteoblast differentiation markers (*RUNX2*, *BMP2*, *COL1* & *OCN*) in an MG63 cell line[40] and Kang *et al.* reported similar osteogenic effects of anionic clays Mg_2Al–Cl and Zn_2Al–Cl on pre-osteoblasts.[41] Similar results have also been reported using other lithium-free clay minerals including Halloysite[42] ($Al_2Si_2O_5(OH)_4{\cdot}nH_2O$), Attapulgite[43] ($(Mg,Al)_2Si_4O_{10}(OH){\cdot}4(H_2O)$) and Imogolite[44] ($(Al_2O_3{-}SiO_2{-}2H_2O)n$).

In conclusion, LAPONITE® nanoparticles are biocompatible and promote early osteogenic activity of HBMSCs. We note, the bioactivity of LAPONITE® does not correlate with lithium content, either as free salts or incorporated in LAPONITE® nanoparticle structures. This suggests against the hypothesised role of lithium release in imparting bioactivity and that other physicochemical features need to be explored to understand the osteogenic effects of LAPONITE® on HBMSCs.

4. Materials & methods

4.1. Human bone marrow stromal cell isolation and culture

Human bone marrow stromal cells (HBMSCs) were isolated from femoral bone marrow aspirate. Bone marrow aspirates were obtained from haematologically normal patients undergoing elective hip replacement surgery at Southampton General Hospital or Spire Hospital Southampton. Only tissue samples that would have been discarded were used following informed consent from the patients in accordance with UK regulations and with approval from Southampton & South West Hampshire Local Research Ethics Committee (LREC 194/99/1). Briefly, HBMSCs were isolated by repeated washes/perfusion of the bone marrow aspirate with α-MEM and centrifugation at 1100 rpm for 5 minutes. The cell pellet resuspended in α-MEM and filtered through 70 μm cell strainer to isolate the cell population from the residual bone chips and remain-

ing unwanted tissues. Cells were seeded at low density (5×10^3 cells per cm^2) in growth medium (α-MEM with supplements of 10% (v/v) FBS and 100 μg ml^{-1} penicillin/streptomycin) and incubated in monolayer at 37 °C and under humidified 5% CO_2 for 3 hours. Culture media change was performed to remove nonadherent cell fraction (red blood cells) while the adherent cells were further grown under the same conditions for 12–14 days, before being passaged for culture expansion. In this way, cells with colony-forming ability were expanded and used in subsequent experiments. Culture medium was changed every 3–4 days. For all experiments, the obtained HBMSCs were used before passage 4.

4.2. LAPONITE® nanoparticles synthesis, modification and characterisation

Standard LAPONITE® SL (SR4871) was provided by BYK-ALTANA. Two classes of lithium-modified LAPONITE® nanoparticles were generated, in collaboration with BYK-ALTANA: structural and exchanged. Briefly, structural lithium refers to lithium incorporated in the octahedral sheet of LAPONITE® crystal while exchanged lithium is adsorbed in the interlayer space and/or on the particle surface (Fig. 3A). Structural lithium was modified by BYK-ALTANA using proprietary methods through tailoring the reactant molar ratios of $SiO_4^{2-} : Mg^{2+} : Li^+ : Na^+$ salts during the initial stages of LAPONITE® crystal synthesis. Standard, null and high structural-lithium LAPONITE® formulations were successfully generated and termed as LAPONITE® SL, NL, HL, respectively.

Exchanged lithium modification was performed through Na^+–Li^+ exchange reaction on the surface of previously synthesised LAPONITE® structures. Briefly, LAPONITE® slurry (filter-cake) was re-heated to 70 °C and filtered on a 24 cm Buchner filter funnel and washed twice with DI water. This was followed by 4 times washing of the filter-cake using 15% Li_2SiO_4 solution at the same temperature. This allowed the Na^+–Li^+ cation exchange reaction to take place between Li^+ in the Li_2SiO_4 solution and Na^+ in the interlayer space of LAPONITE® particles. To remove excess cations from the reaction mixture, the filter-cake was washed several times with DI water, until reaching the conductivity plateaux. Next, the filter-cake was removed from the filter paper and dried on a glass dish in an oven at 110 °C overnight. Finally, the dried product was milled in a Janke and Kunkel A10 mill to a fine white powder.

To investigate LAPONITE® crystal structure for phase transformation or crystal defects, samples underwent powder X-ray diffraction (PXRD) analysis. PXRD experiments were carried out with Bruker D2 Phaser diffractometer using CuKα radiation (λ = 1.5415 Å). The XRD patterns were recorded over the 5°–70° 2θ range using a step of 0.02° and a counting time of 0.3 s per step.

X-ray fluorescence spectroscopy (XRF) was used to measure elemental composition, in the form of oxides, of the as-prepared LAPONITE® structures. However, XRF is less useful for measurement of elements with atomic number $Z < 11$, as in the case of lithium, due to weak fluorescence from these species. Therefore, lithium content was analyzed by atomic absorption spectroscopy (AAS).

4.3. Preparation of LAPONITE® dispersion in cell culture medium

Freshly prepared LAPONITE® dispersions were used for all experiments. Briefly, LAPONITE® powder was sterilised using Blak-Ray B-100AP High intensity UV Lamp (UVP, Upland, CA, USA), then dispersed in sterile-filtered d-H_2O (18.2 MΩ) at a concentration of 0.5% (w/v), before being applied to cell culture media. Cell culture media (basal or osteogenic) was allowed to stir at 700 rpm forming a vortex then LAPONITE®/H_2O solution was added in a very slow manner, to avoid particle agglomeration, up to a final conc. of 1 mg mL^{-1}. For negative controls, LAPONITE®-free H_2O was added. The resultant LAPONITE® dispersions in cell culture media were allowed to stir for 30 minutes before being diluted to the appropriate concentration in media and applied to cells. Basal media consisted of α-MEM (Lonza) containing 10% FBS and 100 μg ml^{-1} penicillin/streptomycin (Sigma), while osteogenic media was prepared of basal media supplemented with 100 μM ascorbate-2-phosphate, 10 mM β-glycerophosphate and 10 nM dexamethasone (Sigma).

4.4. Effect of LAPONITE® on cell viability, adhesion and proliferation

LAPONITE® cytotoxicity was determined using WST-1 colorimetric assay (Roche, Germany). The technique is based on the cleavage of tetrazolium salts to formazan dye by mitochondrial dehydrogenases produced by viable cells. Cells were seeded in clear flat-bottom 96-well plates at varying densities of 1.5×10^3–12×10^3 cells per cm^2 in basal medium and allowed to adhere for 24 hours at 37 °C and 5% CO_2. Next, existing culture media was changed with fresh basal media supplemented with LAPONITE® nanoparticles at a final conc. of 0–1000 μg mL^{-1}. After 24 hours incubation, 10 μL WST1 reagent was added for each well and incubated for 1 hour. The absorbance was measured using EL-800 Universal Microplate Reader (BioTek Instruments Inc., Winooski, USA) at 450 nm. The absorbance/color intensity produced by formazan product correlates with the number of viable cells in the samples.

Cell proliferation was determined using Quant-it™ PicoGreen® dsDNA quantification assay (Invitrogen LifeTech) according to the manufacturer's protocol. Cells were plated at 10^4 cells per cm^2 and allowed to adhere overnight before being treated with 100 μg mL^{-1} LAPONITE® in basal medium and cultured over two weeks at 37 °C in 5% CO_2. At each selected timepoint, cells were washed twice with DPBS and lysed in CelLytic M (Sigma C2978) followed by centrifugation at 12 000*g* for 15 minutes to separate unwanted cell debris from the protein-containing supernatant which was used for ALP activity assay and dsDNA quantification. dsDNA standards were prepared at conc. 0–1000 ng mL^{-1}. Standards (100 μl/ per well) and samples (20 μl/ per well) were pipetted in triplicates in black, 96-well plate then diluted with 80 μl/ per well 1× TE buffer (Tris/EDTA, Sigma). Next, 100 μl/ per well of 0.5%

PicoGreen in 1× TE buffer was added followed by incubation for 5 minutes at room temperature in the dark. Fluorescence was measured using FLx800 fluorescence microplate reader (Biotek) at an excitation/emission of 480/520 nm. dsDNA conc. was read from the standard curve.

4.5. Effect of LAPONITE® on HBMSC osteogenic differentiation

Upon reaching 70–80% confluence, HBMSCs were seeded at a density of 10^4 cells per cm^2 in basal medium and allowed to adhere under 37 °C and 5% CO_2 conditions for 24 hours. To assess the osteogenic potential of standard and lithium modified LAPONITE® structures on HBMSCs, existing medium was replaced with basal or osteogenic culture medium containing 100 μg mL^{-1} LAPONITE® nanoparticles prepared as described above. For negative control LAPONITE®-free medium was used. In all studies HBMSCs were cultured with LAPONITE® nanoparticles for up to 7 days before the first media change or until harvest for analysis. After the first 7-day period, media changes were performed every 3–4 days with LAPONITE®-free media.

To test the effect of LAPONITE® degradation products on alkaline phosphatase activity HBMSCs were incubated with osteogenic culture media supplemented with LiCl, $MgSO_4$ and Na_2SiO_3 salt solutions at concentrations that provide Li, Mg and Si ions at equivalent concentrations to those present in LAPONITE® particles added at 0, 25, 50 and 100 μg mL^{-1}. Standard LAPONITE® powder was used at the same nanoclay conc. (0, 25, 50 & 100 μg mL^{-1}) as a positive control and equivalent concentrations of control salts (NaCl and Na_2SO_4) were also tested to control for any background effects of the test salt counterions (Na^+, Cl^- & SO_4^{2-}). All additives were dissolved in plain alpha MEM and then diluted to the required final ion concentration in osteogenic media. Salt concentrations are provided in Table S1 in ESI.† Following 24 hours incubation of HBMSCs in basal medium, existing medium was replaced with osteogenic media containing LAPONITE®, Li, Mg and Si salts and incubated for 3 days when ALP activity was assayed.

4.5.1. Alkaline phosphatase activity and staining. ALP activity was quantified using an end-point colorimetric assay based on conversion of *p*-nitrophenol phosphate (pNPP) to yellow *p*-nitrophenol (pNP) by ALP enzyme. On day 1, 3, 7, & 14 cell lysates were collected as described previously for dsDNA quantification. Then, 20 μL of the supernatant/lysate from each sample was added in triplicates in clear, flat-bottom, 96-well plate and mixed with 80 μL of 3.6 mM phosphatase substrate (Sigma P47441G). The plate was incubated at 37 °C for 60 minutes in the dark. At the time of colour change, the reaction between ALP and its substrate was stopped by adding 1 M NaOH (100 μL per well). The colour intensity/absorbance was measured using ELx800 microplate reader (BioTek, Winooski, USA) at 415 nm. A standard curve was performed using 4-nitrophenol (Sigma N7660-100ML), which is end product of ALP enzymatic reaction. The ALP activity was calculated as conc. of product/hour based on the obtained absorbance, standard curve and incubation time then normalized to the corresponding DNA content assayed above.

For ALP staining, cells washed twice with DPBS and fixed with 95% ethanol at 4 °C for 10 minutes. Next, naphthol AS-MX phosphate (Sigma 85-5) at 1/25 dilution in dH_2O and fast violet salt (Sigma F1631) at final concentration 0.24 mg mL^{-1} was added and plate incubated at 37 °C for 60 minutes in the dark. Reaction stopped with dH_2O and the cells were imaged using: (1) Carl Zeiss Axiovert 200 microscope with AxioVision imaging software (Zeiss) and (2) Zeiss Stemi 2000 microscope with Canon Power Shot G10 digital camera.

4.5.2. Extracellular matrix mineralisation. Calcium mineralisation in extracellular matrix was determined using alizarin red dye which binds selectively to calcium slats and is widely used for calcium histochemistry. Cells washed twice with DPBS (without Ca^{2+} or Mg^{2+}), and fixed in 4% (w/v) paraformaldehyde for 15 minutes at room temp. Then, fixed cells were incubated with 2% ARS (pH = 4.1–4.3) at room temperature in the dark for 20 minutes. Cells washed several times with dH_2O to remove excess un-bound dye and imaged using (1) Carl Zeiss Axiovert 200 microscope with AxioVision imaging software (Zeiss) and (2) Zeiss Stemi 2000 microscope with Canon Power Shot G10 digital camera.

4.5.3. Real-time quantitative PCR. RT-qPCR was performed to evaluate the mRNA expression of osteogenic genes in response to LAPONITE® addition. First, total RNA was extracted using ISOLATE II RNA Mini Kit (Bioline, BOI-52073) according to the manufacturer's protocol. First-stranded complementary DNA (cDNA) synthesis was performed using TaqMan Reverse Transcription kit (Applied Biosystems, N8080234) on a Mastercycler Gradient (Eppendorf) with a total reaction volume of 20 μL.

Expression of genes of interest was quantified by RT-qPCR using Applied Biosystems reagents and AB7500 cycler. For each sample, 1 μl cDNA was mixed with 19 μl primer mix for a total reaction volume of 20 μl. Reactions were performed in the AB7500 Applied Biosystems cycler (Foster, USA) with the following settings: 50 °C for 2 minutes, 95 °C for 10 minutes, followed by 40 cycles of 95 °C for 15 seconds and 60 °C for 60 seconds. Each sample was run in triplicates and relative expression of target genes was calculated using the $2^{-\Delta\Delta Ct}$ method by normalising first against a reference gene (*ACTB*) then against corresponding negative control (*e.g.* LAPONITE®-free sample). All primers used in this project were designed and validated by Bone & Joint research group at the University of Southampton. Details of primer sequences are included in Table 1.

4.6. Luciferase activity assay

Luciferase assay was performed using engineered 3T3 mouse fibroblast cell line (ENZ-61001-0001, Enzo Life Sciences), which expresses the firefly luciferase reporter gene under the control of Wnt-responsive promoters (TCF/LEF). Cells were seeded in white clear-bottom 96-well plates at density of 1.5×10^4 cells in assay medium (DMEM, 25 mM HEPES (pH = 7.2–7.4), 5% FBS and 0.5% penicillin/streptomycin). Next day,

Table 1 Primer sequences used for RTPCR analysis

Gene name	Forward primer sequence (5′-3′)	Reverse primer sequence (5′-3′)	Product length (bp)
ACTB	GGCATCCTCACCCTGAAGTA	AGGTGTGGTGCCAGATTTTC	82
GAPDH	GACAGTCAGCCGCATCTTCTT	TCCGTTGACTCCGACCTTCA	86
RUNX2	GTAGATGGACCTCGGGAACC	GAGGCGGTCAGAGAACAAAC	78
SP7	ATGGGCTCCTTTCACCTG	GGGAAAAGGGAGGGTAATC	75
ALPL	GGAACTCCTGACCCTTGACC	TCCTGTTCAGCTCGTACTGC	86
COL1A1	GAGTGCTGTCCCGTCTGC	TTTCTTGGTCGGTGGGTG	52
BGLAP	GGCAGCGAGGTAGTGAAGAG	CTCACACACCTCCCTCCT	102
SPP1	GTTTGCGAGACCTGACATCC	CATTCAACTCCTCGCTTTCC	80
AXIN2	CAAGGGCCAGGTCACCAA	CCCCCAACCCATCTTCGT	68

LAPONITE® and LiCl in DMEM were added for final LAPONITE® and LiCl concentrations of 1–100 μg mL^{-1} and 6.25–50 mM, respectively. Samples were run in triplicates and incubated at 37 °C and 5% CO_2 for 18 hours. Then added 100 μl per well luciferase substrate diluted in luciferase buffer (Steady-Glo, Promega, Madison, USA) and incubated at room temperature for 10 minutes in dark. The chemiluminescence signal was immediately read (0.1 second per well) on a Varioscan Flash microplate reader (Thermo Scientific).

4.7. Statistical analysis

All statistical analysis was performed using GraphPad Prism 8.4.3. Data in graphs are expressed as the mean ± SD. All experiments were performed in triplicate using cells from a single donor source. Comparisons between experiment groups were performed using one-way ANOVA, or two-way ANOVA if a time-course experiment was undertaken. Tukey's multiple comparisons test was used to determine significant differences between groups, where significance is set at $P < 0.05$. For all experiments, normality was confirmed by qualitative assessment of the distribution of residuals across all groups of each dataset by analysing the relevant QQ Plots. For RT PCR data lognormal distributions were also assessed, but in the absence of any clear improvement to the normality of the residuals, untransformed data was used for analysis.

Conflicts of interest

Jonathan Dawson and Richard Oreffo are founders of and shareholders in Renovos Biologics Ltd, a University of Southampton spin-out company seeking to commercialise the application of nanoclay in regenerative medicine. Oscar Kelly and Jane Doyle are current employees of the manufacturer of LAPONITE®, BYK-ALTANA Ltd. The remaining authors declare no competing interests.

Acknowledgements

This work was supported by Jonathan Dawson's EPSRC fellowship (grant number EP/L010259/1), the University of Southampton Faculty of Medicine HEIF Enterprise fund and a Regenerative Medicine Platform Acellular/Smart Materials—3D Architecture (MR/R015651/1) grant to Dawson, Evans and Oreffo. Mohamed Mousa would like to acknowledge PhD funding from BYK Additives and the Faculty of Engineering and the Environment, University of Southampton. The authors would like to thank Ms. Julia Wells of the University of Southampton Bone and Joint group for technical support and Dr Yanghee Kim and Dr Roxanna Ramnarine Sanchez for helpful discussions and critical feedback on the results.

References

1 M. Mousa, N. D. Evans, R. O. Oreffo and J. I. Dawson, *Biomaterials*, 2018, **159**, 204–214.
2 A. K. Gaharwar, S. M. Mihaila, A. Swami, A. Patel, S. Sant, R. L. Reis, A. P. Marques, M. E. Gomes and A. Khademhosseini, *Adv. Mater.*, 2013, **25**, 3329–3336.
3 S. M. Mihaila, A. K. Gaharwar, R. L. Reis, A. Khademhosseini, A. P. Marques and M. E. Gomes, *Biomaterials*, 2014, **35**, 9087–9099.
4 S. Wang, R. Castro, X. An, C. Song, Y. Luo, M. Shen, H. Tomás, M. Zhu and X. Shi, *J. Mater. Chem.*, 1391, **22**, 23357–23367.
5 D. Su, L. Jiang, X. Chen, J. Dong and Z. Shao, *ACS Appl. Mater. Interfaces*, 2016, **8**, 9619–9628.
6 F. Topuz, A. Nadernezhad, O. S. Caliskan, Y. Z. Menceloglu and B. Koc, *Carbohydr. Polym.*, 2018, **201**, 105–112.
7 T. Ahlfeld, G. Cidonio, D. Kilian, S. Duin, A. R. Akkineni, J. I. Dawson, S. Yang, A. Lode, R. O. C. Oreffo and M. Gelinsky, *Biofabrication*, 2017, **9**, 034103.
8 L. Tang, W. Wei, X. Wang, J. Qian, J. Li, A. He, L. Yang, X. Jiang, X. Li and J. Wei, *RSC Adv.*, 2018, **8**, 10794–10805.
9 D. W. Thompson and J. T. Butterworth, *J. Colloid Interface Sci.*, 1992, **151**, 236–243.
10 S. Jatav and Y. M. Joshi, *Appl. Clay Sci.*, 2014, **97**, 72–77.
11 D. M. Reffitt, N. Ogston, R. Jugdaohsingh, H. F. J. Cheung, B. A. J. Evans, R. P. H. Thompson, J. J. Powell and G. N. Hampson, *Bone*, 2003, **32**, 127–135.
12 S. Yoshizawa, A. Brown, A. Barchowsky and C. Sfeir, *Acta Biomater.*, 2014, **10**, 2834–2842.
13 P. Cheng, P. Han, C. Zhao, S. Zhang, H. Wu, J. Ni, P. Hou, Y. Zhang, J. Liu and H. Xu, *Biomaterials*, 2016, **81**, 14–26.

14 H. Zreiqat, C. R. Howlett, A. Zannettino, P. Evans, G. Schulze-Tanzil, C. Knabe and M. Shakibaei, *J. Biomed. Mater. Res.*, 2002, **62**, 175–184.
15 W. Wang and K. W. Yeung, *Bioact. Mater.*, 2017, **2**, 224–247.
16 P. Habibovic and J. E. Barralet, *Acta Biomater.*, 2011, **7**, 3013–3026.
17 A. Zamani, G. R. Omrani and M. M. Nasab, *Bone*, 2009, **44**, 331–334.
18 I. Wilting, F. de Vries, B. M. Thio, C. Cooper, E. R. Heerdink, H. G. Leufkens, W. A. Nolen, A. C. Egberts and T. P. van Staa, *Bone*, 2007, **40**, 1252–1258.
19 Y. Jin, L. Xu, X. Hu, S. Liao, J. L. Pathak and J. Liu, *J. Bone Miner. Metab.*, 2017, **35**, 497–503.
20 J. De Boer, H. J. Wang and C. Van Blitterswijk, *Tissue Eng.*, 2004, **10**, 393–401.
21 L. Tang, Y. Chen, F. Pei and H. Zhang, *Cell. Physiol. Biochem.*, 2015, **37**, 143–152.
22 L. Li, X. Peng, Y. Qin, R. Wang, J. Tang, X. Cui, T. Wang, W. Liu, H. Pan and B. Li, *Sci. Rep.*, 2017, **7**, 1–12.
23 P. Han, M. Xu, J. Chang, N. Chakravorty, C. Wu and Y. Xiao, *Biomater. Sci.*, 2014, **2**, 1230–1243.
24 Y. Wu, S. Zhu, C. Wu, P. Lu, C. Hu, S. Xiong, J. Chang, B. C. Heng, Y. Xiao and H. W. Ouyang, *Adv. Funct. Mater.*, 2014, **24**, 4473–4483.
25 C. M. Hedgepeth, L. J. Conrad, J. Zhang, H.-C. Huang, V. M. Lee and P. S. Klein, *Dev. Biol.*, 1997, **185**, 82–91.
26 J. H. Kim, X. Liu, J. Wang, X. Chen, H. Zhang, S. H. Kim, J. Cui, R. Li, W. Zhang and Y. Kong, *Ther. Adv. Musculoskeletal Dis.*, 2013, **5**, 13–31.
27 L. H. Hoeppner, F. J. Secreto and J. J. Westendorf, *Expert Opin. Ther. Targets*, 2009, **13**, 485–496.
28 A. A. Janeczek, R. S. Tare, E. Scarpa, I. Moreno-Jimenez, C. A. Rowland, D. Jenner, T. A. Newman, R. O. Oreffo and N. D. Evans, *Stem Cells*, 2016, **34**, 418–430.
29 A. A. Janeczek, E. Scarpa, M. H. Horrocks, R. S. Tare, C. A. Rowland, D. Jenner, T. A. Newman, R. O. Oreffo, S. F. Lee and N. D. Evans, *Nanomedicine*, 2017, **12**, 845–863.
30 N. Von Moos, P. Bowen and V. I. Slaveykova, *Environ. Sci.: Nano*, 2014, **1**, 214–232.
31 J. K. Carrow, L. M. Cross, R. W. Reese, M. K. Jaiswal, C. A. Gregory, R. Kaunas, I. Singh and A. K. Gaharwar, *Proc. Natl. Acad. Sci. U. S. A.*, 2018, **115**, E3905–E3913.
32 T. Li, Z. L. Liu, M. Xiao, Z. Z. Yang, M. Z. Peng, C. D. Li, X. J. Zhou and J. W. Wang, *Stem Cell Res. Ther.*, 2018, **9**, 100.
33 J. R. Xavier, T. Thakur, P. Desai, M. K. Jaiswal, N. Sears, E. Cosgriff-Hernandez, R. Kaunas and A. K. Gaharwar, *ACS Nano*, 2015, **9**, 3109–3118.
34 P. Kerativitayanan, M. Tatullo, M. Khariton, P. Joshi, B. Perniconi and A. K. Gaharwar, *ACS Biomater. Sci. Eng.*, 2017, **3**, 590–600.
35 A. Paul, V. Manoharan, D. Krafft, A. Assmann, J. A. Uquillas, S. R. Shin, A. Hasan, M. A. Hussain, A. Memic, A. K. Gaharwar and A. Khademhosseini, *J. Mater. Chem. B*, 2016, **4**, 3544–3554.
36 B. O. Okesola, S. Ni, B. Derkus, C. C. Galeano, A. Hasan, Y. Wu, J. Ramis, L. Buttery, J. I. Dawson and M. D'Este, *Adv. Funct. Mater.*, 2020, **30**, 1906205.
37 J. Li, Z. Khavandgar, S.-H. Lin and M. Murshed, *Bone*, 2011, **48**, 321–331.
38 P. S. Klein and D. A. Melton, *Proc. Natl. Acad. Sci. U. S. A.*, 1996, **93**, 8455–8459.
39 V. Stambolic, L. Ruel and J. R. Woodgett, *Curr. Biol.*, 1996, **6**, 1664–1669.
40 G.-J. Kim, D. Kim, K.-J. Lee, D. Kim, K.-H. Chung, J. W. Choi and J. H. An, *Nanomaterials*, 2020, **10**, 230.
41 H. R. Kang, C. J. da Costa Fernandes, R. A. da Silva, V. R. L. Constantino, I. H. J. Koh and W. F. Zambuzzi, *Adv. Healthcare Mater.*, 2018, **7**, 1700693.
42 G. Nitya, G. T. Nair, U. Mony, K. P. Chennazhi and S. V. Nair, *J. Mater. Sci. Mater. Med.*, 2012, **23**, 1749–1761.
43 Z. Wang, Y. Zhao, Y. Luo, S. Wang, M. Shen, H. Tomás, M. Zhu and X. Shi, *RSC Adv.*, 2015, **5**, 2383–2391.
44 K. Ishikawa, T. Akasaka, Y. Yawaka and F. Watari, *J. Biomed. Nanotechnol.*, 2010, **6**, 59–65.